This study investigates how dust aerosols influence precipitation in China using an improved online aerosol–ice-nucleation (aerosol-IN) scheme implemented in the GRAPES/CUACE regional model. The topic is interesting and important in the field of aerosol–cloud–precipitation interactions. However, in many parts of the manuscript, the authors draw conclusions without sufficient observational evidence. This is the major drawback of the study. Therefore, I am on the negative side regarding publication of this paper.

General Comments

Dear editor and reviewers,

Thank you for your thorough review of the manuscript. We have read the reviewer's comments carefully, and have responded and taken your comments into consideration and revised the manuscript accordingly. All the changes have been highlighted in the revised manuscript. Our detailed responses, including a point-by-point response to the reviews and a list of all relevant changes, are as follows:

1. Lack of observational analysis:

As mentioned in the overall assessment, this paper lacks observational analysis to support its conclusions. For example, in lines 317–321, the authors should evaluate model results against radar observations and include water and/or ice saturation information. In line 349, observational evidence for the mass ratio between cloud ice and snow (1:3) should be presented to justify its alignment with observations, as this ratio can vary from case to case. For lines 431–432, there is no analysis or evidence explaining the underestimation of ice nuclei concentrations in the original WDM6 scheme.

A: Thank you for your careful review of the manuscript. You are correct that direct observations of in-cloud microphysical processes during dust events are extremely difficult to obtain, and many existing studies rely on laboratory experiments to infer microphysical changes under controlled temperature and humidity conditions. In our revision, we have made efforts to validate the model

behavior using available observational evidence from previous field and laboratory studies.

For example, in lines 317–321, the authors should evaluate model results against radar observations and include water and/or ice saturation information.

A: Available aircraft and modeling studies indicate that ice-nucleating particles (INPs) and ice-phase hydrometeors tend to concentrate at mid-to-upper tropospheric levels, but their vertical distribution strongly depends on season and thermodynamic conditions, rather than occurring universally near the homogeneous freezing level (−40 °C).

For example, aircraft observations by (He et al., 2023) during non-dust autumn conditions showed peak INP concentrations around 4–5 km, while (Zhang et al., 2021) simulated summertime dust–precipitation in Taiwan interactions and found enhanced ice-phase hydrometeors mainly between 0 and −20 ℃ (approximately 7–8 km).

These studies suggest that the vertical location of maximum ice-phase activity varies substantially across cases. In contrast, the original WDM6 scheme produces a systematic maximum near −40 ℃, which appears inconsistent with both observational and modeling evidence under springtime dust conditions. Our revised scheme shifts the dominant ice-phase production to warmer levels, which is more physically plausible for spring dust–precipitation events.

in line 349, observational evidence for the mass ratio between cloud ice and snow (1:3) should be presented to justify its alignment with observations, as this ratio can vary from case to case.

A: Direct observational separation of cloud ice and snow mass is indeed challenging, because radar reflectivity from larger snow particles often masks the

signal from small ice crystals (Kedzuf et al., 2021). Nevertheless, existing aircraft and in situ observations consistently indicate that cloud ice typically has higher number concentrations but lower mass compared with snow (Lawson et al., 2001; Wang et al., 2023). This qualitative relationship is also reproduced in previous modeling studies. This fundamental relationship is reproduced in models, and our chosen ratio of 1:3 is consistent with the range of values reported in prior observationally constrained modeling studies. For instance, Park and Lim (2023)reported a ratio near 1:3, while Zhang et al. (2021) found a ratio close to 1:5 in mid-latitude mixed-phase clouds influenced by dust.

Our simulated ratio (1:3) therefore lies within the range documented by prior observationally constrained studies.

For lines 431–432, there is no analysis or evidence explaining the underestimation of ice nuclei concentrations in the original WDM6 scheme.

A: We agree with the reviewer that observational evidence is important for demonstrating the underestimation of IN concentrations in the original WDM6 scheme. Although direct in-cloud INP measurements during dust events are limited, multiple independent field and laboratory studies in East Asia show that dust outbreaks substantially enhance INP concentrations for heterogeneous freezing.

Bi et al. (2019) reported IN concentrations up to 2800 L^{-1}during dust-influenced days in May–June 2018 at −20℃ to −30 ℃ using a continuous-flow diffusion chamber in Beijing.

Chen et al. (2021) measured immersion-mode INPs at Peking University Atmosphere Environment Monitoring Station during spring 2018–2019 and found that dust periods increased INP concentrations by approximately two orders of magnitude, reaching 10 $^{2}L^{-1}$between −15℃ and −28℃.

Hu et al. (2023) reported INP concentrations near 10 $^{3}L^{-1}$at −20 °C at two contrasting northern China sites (a polluted urban site and a clean mountain site), indicating that dust significantly elevates INPs across very different environments.

Measurements of Tobo et al. (2019) at the Tokyo Skytree showed that during transported dust events, immersion-mode IN reached 10 $^{2}L^{-1}$, confirming that dust strongly enhances IN even far downstream of the source.

Across these studies, heterogeneous INP concentrations during East Asian dust events typically fall in the range of 10 ^{2}–10 $^{3}L^{-1}$at temperatures.

In contrast, the original WDM6 parameterization produces IN concentrations of only 10^{0}–10 $^{1}L^{-1}$, and shows little distinction between dust and non-dust periods. This mismatch demonstrates that the original WDM6 scheme substantially underestimates heterogeneous IN activation, which is consistent with the reviewer's concern.

2. Incorrect or missing references:

In several places, the manuscript either lacks proper references for the physical parameterizations used or cites incorrect previous studies. For instance, Park and Lim (2023) and Kwon et al. (2023) did not evaluate their results using MODIS observations, contrary to what is stated in line 94. The statement in lines 99–104 is also incorrect. The authors should carefully review and cite previous studies throughout the manuscript. Furthermore, Hong et al. (2006) is not the correct reference for the WDM6 scheme (line 155); the appropriate citation is Lim and Hong (2010).

A: We have thoroughly re-examined all citations within the manuscript and have corrected the issues pertaining to incorrect or missing references.

In line 99-102:

Moreover, many clouds ice microphysical schemes were single-moment, which only simulated the mass mixing ratio of cloud ice. Such single-moment schemes often led to large biases in cloud ice mass concentrations (Molthan and Colle, 2012; Igel et

al., 2015). In contrast, double-moment ice schemes, which simulate both cloud ice mass and number concentrations, outperform the single-moment schemes in terms of the simulated structure, life cycle, cloud coverage, precipitation, and microphysical properties (Pu and Lin, 2015; Zhao et al., 2021).

In line 110-114:

Park and Lim (2023) develops the revised Weather Research and Forecasting Double-Moment 6-class (WDM6) scheme through the implementation of prognostic cloud ice number concentrations. The excess generation of cloud ice mixing ratio is considerably alleviated.

3. Need for microphysical budget analysis:

To draw reliable conclusions about the vertical profiles of hydrometeors, the authors need to perform a detailed microphysics budget analysis. For example, they argue that increased cloud ice enhances accretion by snow, converting cloud ice to snow. However, this cannot be concluded without budget diagnostics, as other processes—such as aggregation of cloud ice or accretion of snow by rain—could also contribute. I strongly recommend that the authors conduct budget analyses for different stages of precipitation development.

A: We appreciate the reviewer's suggestion and fully agree that microphysical budget analysis is essential for drawing robust conclusions.

Following this recommendation, we conducted detailed budget diagnostics for cloud ice, snow, cloud water, and rainwater at different vertical layers corresponding to different thermodynamic regimes.

Based on the variation characteristics, the vertical layer is divided into three parts: layer A, above 7 km (temperature below −18 °C); layer B, between 4 and 7 km (temperature approximately −18 °C to -1.5 ℃); and layer C, below 4 km (temperature approximately -1.5 ℃ to 18 ℃).

These budget analyses have been added to the revised manuscript in Section 3.2：

During the DP event, the introduction of the on-line aerosol-IN nucleation scheme allows dust aerosols to alter the distribution of cloud hydrometeors. Figure 3 shows the DP-event-averaged vertical distributions of hydrometeors in T_CTL and T_IN, as well as their difference (T_IN − T_CTL), by using budget analysis. Figure 4 shows the differences in the production rates of different hydrometeors (T_IN − T_CTL).

Cloud ice

In layer A, when dust aerosols are considered, the IN number concentration decreases in T_IN (Fig. 2c), resulting in cloud ice number concentrations in T_IN that are approximately 5 L^{-1} lower than those in T_CTL, about 40% of T_CTL (Fig. 3d). The cloud ice mass concentration is reduced to only 10% – 50% of T_CTL (Fig. 3a,3b). Because the two primary processes contributing to cloud ice formation in this layer—heterogeneous nucleation and deposition-sublimation of cloud ice —are both suppressed (Fig. 4a), and the total production rate of cloud ice (Pigen+Pidep-Psaut-Praci-Psaci-Pgaci) drops to less than 24% of that in T_CTL. On the one hand, the nucleated IN number concentration decreases, weakening the Pigen in T_IN by 1–2 orders of magnitude relative to T_CTL. On the other hand, the reduction in cloud ice number concentration allows the ice crystals to grow more efficiently, with their effective particle size generally reaching 98%-135% of that in T_CTL. The combined effect of these two factors ultimately limits the deposition of water vapor onto the ice crystals. Consequently, Pidep decreases to 20%–50% of T_CTL, with the maximum suppression occurring at approximately 7–8 km (Fig. 4a).

In layer B, cloud ice number concentrations in T_IN range from 7 to 10 L^{-1}, approximately 120% of those in T_CTL. However, the cloud ice mass concentration in T_IN is reduced to only 70%–90% of T_CTL. The effective diameters of cloud ice

also decrease to only 77%–97% of T_CTL, with occasional reductions exceeding 50%. This reduction is mainly attributable to combined effects of enhanced heterogeneous nucleation and suppressed depositional growth, and the total production rate of cloud ice drops to less than 82% of that in T_CTL. Dust aerosols provide additional ice nuclei, leading to a substantial enhancement of heterogeneous nucleation in T_IN and the formation of a much larger number of newly formed small ice crystals, with Pigen exceeding that in T_CTL by more than two orders of magnitude. However, the increase in cloud ice number concentration is accompanied by a reduction in individual particle size, which limits the deposition of water vapor onto ice crystals. As a result, Pidep in T_IN is reduced to about 30% of that in T_CTL, indicating that growth of cloud ice via depositional processes is inhibited.

Snow

In layer A, the total snow production rate in T_IN increases to approximately 88% -200% of that in T_CTL (Psdep+Paacw+Psaut+Piacr+Praci+Psaci+Psacr-Pgaut-Pracs, Fig. 4b), leading to an increase in snow mass concentration to 120%–200% of T_CTL (Fig. 3a, 3b). This increase results from the combined effects of enhanced production rate for deposition-sublimation of snow (Psdep) and weakened production rate for aggregation of cloud ice to snow (Psaut) and production rate for accretion of cloud ice by snow (Psaci). The Psdep can reach approximately 2–5 times that in T_CTL (Fig. 4b). In WDM6, the deposition growth of ice-phase hydrometeors is constrained by the available water vapor, with cloud ice deposition given priority and snow deposition consuming the remaining vapor. Because Pidep is reduced to about 20%–50% of that in T_CTL, more water vapor is allocated to snow deposition, Psdep is then enhanced. Meanwhile, as cloud ice reduces, Psaut and Psaci are weakened in T_IN, with both processes reduced to approximately 40%–60% of their values in T_CTL (Fig. 4a, 4b). Despite the suppression of these source terms, the substantial enhancement of snow deposition growth dominates the snow budget in layer A, resulting in a net increase in snow production and cloud-snow mass concentration.

Finally, the ratio of cloud ice to cloud snow changes from 1:1 to 1:3 in layer A, more closely consistent with observation, which shows that cloud ice generally has higher number concentrations but lower mass concentrations than cloud snow (Gao et al., 2020; Yang et al., 2021; Feng et al., 2021; Fang et al., 2022).

In layer B, the snow mass concentration shows relatively small changes, ranging from approximately 90% to 100% of T_CTL. From the perspective of cloud microphysics, the mechanisms are similar to those in layer A. Despite the reduction of Pidep, the Psdep increases to 130%–200% of T_CTL. At the same time, the decrease in cloud ice mass leads to the continued suppression of Psaut and Psaci, resulting in a total snow production rate of about 95% of T_CTL.

In layer C, although the model diagnostics indicate an enhancement in cloud-snow production processes (production rate for accretion of rain by snow (Psacr) and production rate for accretion of rain by cloud ice (Piacr)) and a reduction in the production rate for accretion of snow by rain (Pracs), newly formed cloud snow cannot be maintained because the temperature is already above 0 °C which makes it instantaneously melt, rapidly converting to rain. As a result, there is no significant change in snow mass concentration in this layer.

Cloud water and rainwater

Cloud water and rainwater are mainly distributed in layer C (temperature approximately -2 ℃ to 18 ℃). In this layer, both cloud-water and rainwater mixing ratios in T_IN are about 90%-95% of those in T_CTL. This small reduction is primarily attributed to a weakening of the production rate for cloud droplet activation from CCN (Pcact), which decreases by about 5% in T_IN relative to T_CTL, indicating a suppressed conversion of water vapor into liquid water. As a consequence of the reduced cloud-water content, the production rate for accretion of rainwater by cloud water (Pracw) is also weakened, by 5%–10%. Meanwhile, the conversion of rainwater into ice-phase hydrometeors (Psaci, Pgaci, and Piaci) is enhanced.

However, under the thermodynamic conditions of layer C, temperatures exceed the melting thresholds of ice-phase hydrometeors, the newly formed snow and graupel rapidly melt and are easily converted back into rainwater. Consequently, these ice-phase conversion processes contribute only marginally to the net change in rainwater mixing ratio.

Overall, dust suppresses cloud development, reducing the total ice-phase hydrometeor content in layer A to 70 – 85% of T_CTL, the total ice-phase hydrometeor content in layer B to 85 – 91% of T_CTL, and the liquid-phase hydrometeor content in layer C to 90 – 95% of T_CTL. Our results indicate that dust aerosols tend to suppress cloud development in springtime dust-related precipitation over East Asia, where precipitation is predominantly stratiform. Similar suppression effects have also been reported in previous observational studies (Wang et al., 2022b; Zhu et al., 2023).

4. Aerosol–IN nucleation scheme:

A: Thank you for this question. We respond to each point below.

- The authors should explicitly compare the ice nucleation parameterizations used in Park and Lim (2023) and in this study to clarify the differences among T_CTL, T_CCN, and T_IN experiments. A comparative table would be useful. Notably, WDM6 with prognostic cloud ice number concentration (Park and Lim) did not use the formula $\rho qI0(kg\ m-3)$= 4.92 × 10-11$Nice$ 1.33 to calculate nucleation of ice, which is Pigen, indicating all nucleation processes, in Hong et al., (2024). Instead, Park and Lim's version explicitly treats immersion, contact, and deposition nucleation separately.

A: In GRAPES/CUACE, the original WDM6 scheme follows Hong et al. (2004), in which the ice nucleation of cloud ice is parameterized using

$\rho qI0(kg\ m-3)$= 4.92 × 10-11$Nice$ 1.33 which represents the total effect of heterogeneous ice nucleation and is used to diagnose the ice nucleation rate (Pigen). This formulation is still applied in T_CTL.

In contrast, Park and Lim (2023) employed a prognostic ice nucleation framework in which ice nucleation rates are explicitly calculated based on aerosol diffusion coefficients, and different heterogeneous nucleation pathways (immersion, contact, and deposition/condensation freezing) are treated separately. In their formulation, the conversion of production rate of ice nuclei number to production rate of ice mass is expressed as

$$\text{Pinud} = \text{Ninud} \times \frac{4\pi}{3}\frac{\rho_i}{\rho_a}\ Rind^3$$

In this study, the corresponding formulation is

$$P_{inud}(kgkg^{-1}s^{-1}) = \frac{4}{3}\pi\frac{\rho_i}{\rho_a}\ (r_{id}^3 N_{icenud})/\Delta t$$

which is structurally equivalent to that used by Park and Lim (2023). The key difference lies in the treatment of the initial radius of newly nucleated ice crystals. Park and Lim (2023)assumed a fixed initial ice crystal radius of 10 μm, whereas in this study, following Chen et al. (2019), different initial radii are prescribed for immersion freezing and deposition/condensation freezing, reflecting their different growth efficiencies and formation difficulties.

Based on East Asian cloud-ice size observations, we assume:

$$\begin{cases} r_{df=10\ \mu m} (r_{aer}<10\ \mu m) \\ r_{df=30\ \mu m} (r_{aer}>10\ \mu m) \end{cases}$$

$$\begin{cases} r_{if=30\ \mu m}\ \ (r_{aer}<10\ \mu m) \\ r_{if=50\ \mu m}\ \ (r_{aer}>10\ \mu m) \end{cases}$$

Therefore, although the formulations differ in implementation details, the core physical linkage between IN number concentration and ice mass production is consistent between this study and Park and Lim (2023).

- The comparison of IN concentrations between this study and Park and Lim (2023) also needs careful reconsideration. Even though the authors replaced the ice nucleation scheme in WDM6 with the prognostic version, they compare IN concentrations with those from older WDM6 versions (Hong et al., 2024; Lim and Hong, 2010). According to Eqs. (4–6) in Park and Lim (2023), IN concentrations are treated differently for contact versus deposition/condensation processes, even though both are temperature edependent.

A: In the original WDM6 scheme, the IN concentration is parameterized as

$N_{ice}(m^{-3})=10^{3}e^{0.1(T_0-T_k)}$, which represents the total concentration of activated ice nuclei by heterogeneous nucleation. Dividing by the time step (Δt) yields the heterogeneous nucleation rate (Nigen).

In this study, we diagnose the total heterogeneous nucleation rate as Pigen is diagnosed as the sum of Pinui and Pinud. In T_IN, Nigen is diagnosed as the sum of N_{icenud} and N_{icenud}, divided by the time step

Our analysis further shows that immersion freezing is the dominant heterogeneous nucleation mechanism, exceeding deposition and condensation freezing by 4–5 orders of magnitude in DP-event-averaged production rate for nucleated IN number concentration and 5–6 orders of magnitude in production rate of cloud ice. Given this large disparity and for clarity of comparison, we therefore present the heterogeneous nucleation rate (Pigen) consistently in the figures.

- More clarification is needed for their new on-line aerosol-IN nucleation scheme. Does naer,0.5 in Eq.3 represent the same quantity as in Eq. (2)—the number concentration of insoluble aerosol particles larger than 0.5 μm (e.g., dust, black carbon, and some organic carbon)? What is r in Eq. (4)?

A: In Eqs. (2) and (3), naer,0.5 represents the number concentration of insoluble aerosol particles larger than 0.5 μm, including dust, black carbon, and a fraction of organic carbon, following Chen et al.

In Eq. (4), r denotes the initial radius of cloud ice formed via different nucleation pathways: r_{if} represents the initial radius of cloud ice formed by immersion freezing, and r_{df} represents the initial radius of cloud ice formed by deposition and condensation freezing.

These values correspond to the assumed initial cloud-ice sizes based on East Asian observations (Um et al., 2018; Chen et al., 2021; Yang et al., 2021).

5. Physics parameterization references:

The authors should cite appropriate references for the physics parameterizations used in their GRAPES/CUACE configuration (Section 2.2.1).

A: We have thoroughly re-examined all citations within the manuscript and have corrected the issues pertaining to incorrect or missing references.

In line 169-171:

The IN concentration is calculated by a classical ice nuclei nucleation scheme, which is an empirical function of temperature and does not account for the influence of atmospheric aerosols (Hong et al., 2004):

In line 217-223:

The parameterization scheme selected here is developed by Jiang et al. (2016) and (Chen et al., 2019). It first developed by Jiang et al. (2016) based on dust events observed in Xinjiang, Huangshan, and Nanjing in China, using the static vacuum vapor diffusion chamber Frankfurt Ice nucleation Deposition freezing Experiment. Then some parameters of it was refined and extended it to represent both deposition and immersion freezing by Chen et al. (2019) .

6. Support for the downstream transport conclusion: To substantiate the claim that suppressed cloud water is transported downstream in T_IN, supportive figures should be presented.

A: Thank you for this question. The statement regarding downstream transport of suppressed cloud water is not inferred directly from Figures 3 or 4, but from an additional diagnostic analysis of hydrometeor fluxes in Section 3.3.

We calculate horizontal hydrometeor fluxes across 116 ℉, 33 °–50 ℕ and 33 ℕ, 103 °–116 ℉ from 12:00 UTC on 12 April to 18:00 UTC on 13 April (Fig. 6). Over the entire 0–12 km layer, the total hydrometeor flux slightly increases to about 102% of that in T_CTL.

Within the temperature range from 0 to -40 ℃, the total horizontal hydrometeor flux decreases by about 11 %, primarily due to a substantial reduction in cloud ice flux, accompanied by increases in snow and graupel fluxes. In Layer A, the total hydrometeor flux is about 4.4 × 10-5 kg s-1, corresponding to about 75 % of T_CTL. Cloud ice flux drops sharply to about 8 % of T_CTL, while snow and graupel fluxes increase markedly to about 19.8 times and 7.8 times, respectively. In Layer B, the total hydrometeor flux is about 2.6 × 10-6 kg s-1, corresponding to about 93 % of T_CTL, with cloud ice flux reduced to about 28 % of T_CTL, and snow and graupel fluxes increased to about 2.3 times and about 1.8 times, respectively. At temperatures above 0 ℃, the total horizontal hydrometeor flux increases to about 106 % of T_CTL, with cloud water and rainwater fluxes increasing to about 115 % and about 108 %, respectively.

Specific Comments

1. - Line 265:

“As simulation time increases, integration errors tend to accumulate (Zhang et al., 2019), and to minimize the influence of initial conditions on precipitation, an additional test is conducted from 11 to 13 April.” → This sentence is unclear. Did you perform another simulation starting from 11 April? Please clarify.

A: Yes. You are right, we have corrected it.

In line 290-294:

As simulation time increases, integration errors tend to accumulate (Zhang et al., 2019), and to minimize the influence of initial conditions on precipitation, the simulations in this study were divided into several time segments: 5–8 April, 8–11 April, 11–14 April, and 13–16 April. Among these, the simulation results for 13 April were taken from the 11–14 April experiment to minimize the influence of initial conditions on precipitation development.

2. - Line 208:

"It ignores the influence of IN size and heterogeneous ice nucleation processes." → This is incorrect. The formula includes all heterogeneous ice nucleation processes because Nice represents IN concentration.

A: Yes. You are right, Thank you for your comment. The $\mathbf{N_{ice}}$ in the original WDM6 scheme represents the total concentration of nucleated ice nuclei by heterogeneous nucleation. Our intended criticism was not that it ignores the existence of heterogeneous nucleation, but rather that it does not differentiate between the various heterogeneous nucleation mechanisms (e.g., immersion, condensation, and deposition freezing) and their potentially distinct impacts on subsequent ice crystal growth.

We have corrected it in line 224 -230:

WDM6 uses the formula $\rho q_{I0}(kg\ m^{-3}) = 4.92 \times 10^{-11} N_{ice}{}^{1.33}$ and $P_{igen}(kgkg^{-1}s^{-1}) = \frac{(q_{I0}-q_I)}{\Delta t}$ to calculate newly nucleation of ice. Where, ρ denotes the newly-formed air density, and q_{I0} is the predicted ice mixing ratio (kg kg-1). Δt is the integration time step. Production rate for heterogeneous nucleation is calculated as the difference between q_{I0} and the current ice mixing ratio (q_I). However, it does not account for the influence of nucleated IN size or the specific characteristics of different heterogeneous ice nucleation mechanisms on ice crystal development.

3. - Equations (4) and (6):

These appear to be mathematically identical. Please verify.

A: Yes， We have corrected this in the revised manuscript. The redundant equation (previously labeled as Equation (6)) has been removed entirely.

We have corrected it in line 231-235:

In this paper, The mass production rate of cloud ice newly nucleated is calculated using Equation (4):

$$P_{inud}(kgkg^{-1}s^{-1}) = \frac{4}{3}\pi\frac{\rho_i}{\rho_a}\left(r_{df}^3 N_{icenud}\right)/\Delta t \quad (4)$$

$$P_{inui}(kgkg^{-1}s^{-1}) = \frac{4}{3}\pi\frac{\rho_i}{\rho_a}\left(r_{if}^3 N_{icenui}\right)/\Delta t$$

Where, Where, P_{inud} is mass production rate for deposition/condensation freezing， P_{inui} is for immersion freezing. P_{inud} depletes water vapor to form cloud ice, while P_{inui} depletes cloud water to form cloud ice.

4. - Line 233:

Mark the locations of Ningxia, Shanxi, Hebei, etc., in Figure 1.

A: Yes. We have added Supplementary Figure 1 to show the locations of Ningxia, Shanxi, Hebei, and other relevant provinces.

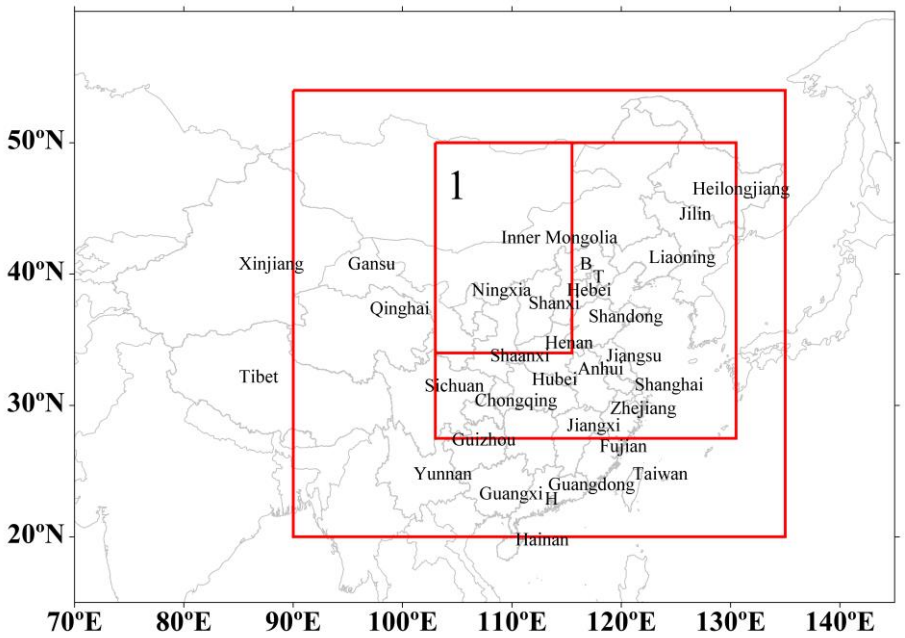

Fig. S1 China Province Map, where B denotes Beijing; T denotes Tianjin; H denotes Hong Kong.

5. - Line 254:

What is the ambient temperature between 3 km and 5 km altitude?

A: Thank you for this important question. The ambient temperatures provided below are the area- and time-averaged values from our model simulation, specifically averaged over the Dust-Precipitation station and during the Dust-Precipitation period. Based on the vertical levels of our GRAPES/CUACE configuration, the interpolated ambient temperatures at the specified altitudes are as follows:

3 km: 275.33 K

4 km: 271.91 K

5 km: 265.30 K

6. - Figure 2 (page 12):

This should be Figure 3.

A: Yes. You are right, we have corrected it.

7. **Why do the authors analyze only one model time step (100 s)? What real time does 100 s correspond to?**

A: Thank you for this important question. The value of 100 s refers specifically to the internal integration time step of the GRAPES model's dynamical core. We recognized that explicitly stating this numerical parameter was unnecessary for interpreting the results of the ice nucleation rate and cloud ice growth rate. In the revised manuscript, we no longer analyze microphysical tendencies over a single model integration time step. Instead, all microphysical processes (heterogeneous nucleation (Pigen) and production rate for deposition- sublimation rate of cloud ice (Pidep)) are expressed consistently in terms of physical rates (e.g., g $kg^{-1}s^{-1}$), which are independent of the model's internal integration time step.

8. **- Line 306–307:**

The authors should show the underestimation of IN concentrations when the online aerosol–IN scheme is not used.

A: Thank you for this important question. Figures 2a and 2b show the maximum nucleated IN number concentration during the dust–precipitation event, while Figure 2c shows the event-averaged vertical distribution. Multiple field and laboratory studies confirm that the nucleated IN concentrations simulated by our improved scheme are consistent with observational and experimental results:

Bi et al. (2019) reported IN concentrations up to 2800 L^{-1} during dust-influenced days in May–June 2018 at −20℃ to −30 ℃ using a continuous-flow diffusion chamber.

Chen et al. (2021) measured immersion-mode INPs at PKUERS during spring 2018–2019 and found that dust periods increased INP concentrations by approximately two orders of magnitude, reaching 10^2 L^{-1} between −15℃ and −28℃.

Hu et al. (2023) reported INP concentrations near 10^3 L^{-1} at −20 °C at two contrasting northern China sites (a polluted urban site and a clean mountain site), indicating that dust significantly elevates INPs across very different environments.

Measurements of Tobo et al. (2019) at the Tokyo Skytree showed that during transported dust events, immersion-mode IN reached 10^2 L^{-1}, confirming that dust strongly enhances IN even far downstream of the source.

In contrast, the original WDM6-based scheme (T_CTL) produces nearly uniform and much lower IN concentrations (around 10^0-10^1 L^{-1}), indicating a systematic underestimation of dust-related IN activity.

We have corrected it in line 239-244:

The on-line aerosol-IN nucleation scheme can correct the systematic underestimation of IN concentrations. The maximum nucleated IN number concentrations in T_CTL can reach 10^2 L-1 in layer B during the DP event (Fig. 2a), showing a relatively uniform horizontal pattern, which is much lower than observed IN concentrations (10^2–10^4 L^{-1}) during East Asian dust events (Bi et al., 2019; Tobo et al., 2019; Chen et al., 2021; Hu et al., 2023).

9. - Line 315: Besides dust, what other aerosol types serve as IN?

A: Thank you for this important question. In addition to dust aerosols, our model also considers black carbon (BC) and a fraction of organic carbon (OC) aerosols to serve as ice-nucleating particles (INPs), following the approach of Chen et al. (2019).

10. - Lines 329–330:

Specify the actual dates and times corresponding to phases 1, 2, and 3.

A: Thank you for this important question.

Because the occurrence time of dust–precipitation coupling varies among observation stations across area 1, we adopt a condition-based compositing approach, focusing on periods when dust and precipitation coexist. Specifically, only time steps and grid points that satisfy $PM_{2.5}/PM_{10} < 0.6$ and surface precipitation greater than 0.1 mm are included in the analysis. This approach allows us to robustly quantify the average microphysical responses to dust across different locations and times.

We have revised the manuscript to clarify that the phases refer to event-based, regional-time averages, not fixed simulation periods in Line 311-315.

Due to the complex sources of PM_{10} and considering the relatively long atmospheric residence time of dust, we select precipitation stations where the $PM_{2.5}/PM_{10}$ ratio is less than 0.6 within 24 hours prior to the precipitation event as representative of dust-influenced precipitation (DP) stations (Wang and Yan, 2007; Filonchyk et al., 2019).

11. - Line 338:

Replace "below 6 km" with "above 4 km."

A: Yes. You are right, we have corrected it.

12. - Line 340:

Why is the cloud-top temperature higher under dusty conditions?

A: We analyzed the microphysical budget terms and the associated temperature tendencies in the cloud layer.

The budget analysis shows that, in the 5–8 km layer, several ice-phase microphysical processes are modified under dusty conditions. Specifically, the conversion of water vapor and rainwater to cloud ice is suppressed, with the corresponding growth rates reduced to less than 50% of those in T_CCN. In contrast,

the conversion of water vapor to snow and graupel is enhanced, reaching approximately 2–3 times that in T_CCN.

However, when these microphysical changes are translated into temperature tendencies, their net contribution to temperature change remains very small. The event-averaged temperature tendency induced by microphysical processes is on the order of -0.002 to -0.001 °C in T_CCN, and about 70% of that magnitude in T_IN. Although these changes may contribute marginally to a slightly higher cloud-top temperature, their magnitude is far too small to be considered the primary driver of the cloud-top temperature increase.

Therefore, we conclude that the higher cloud-top temperature under dusty conditions is not mainly controlled by cloud microphysical processes, but likely reflects the combined effects of large-scale thermodynamic conditions and dynamical adjustments, while microphysical effects play only a secondary role. Finally, the discussion on cloud-top temperature has been removed from this paper.

13. - Line 350:

Include analysis of hydrometeor number concentrations as well.

A: Yes. In the revised manuscript, we have included an explicit analysis of hydrometeor number concentrations by taking advantage of the double-moment cloud-ice representation. The corresponding results are presented in Section 3.2.

Above 7 km, when dust aerosols are considered, the IN number concentration decreases in T_IN (Fig. 2c), leading to cloud-ice number concentrations that are approximately 5 L^{-1} lower than those in T_CTL, corresponding to about 40% of T_CTL (Fig. 3d). Meanwhile, the cloud-ice mass concentration is reduced more substantially, to only 10% – 50% of that in T_CTL (Fig. 3a,b).

In contrast, within the 4–6 km layer, dust aerosols provide additional ice-nucleating particles, increasing cloud-ice number concentrations in T_IN to 7–10 L^{-1}, which is about 120% of T_CTL. However, the cloud-ice mass concentration in this layer is still reduced to 70%–90% of T_CTL. Consistently, the effective diameter of cloud ice decreases to 77%–97% of that in T_CTL, with occasional reductions exceeding 50%.

These results indicate that changes in cloud-ice mass are not solely controlled by number concentration, but also strongly modulated by particle growth efficiency.

14. - Lines 361–362:

Check this sentence for clarity and correctness.

A: Following the reviewer's suggestion, we have substantially revised the analysis by (1) increasing the model output frequency from 3 h to 1 h and (2) introducing a detailed microphysical budget analysis focused on dust–precipitation periods. As a result, the analytical framework of Section 3 has changed from a comparison between pre-dust and post-dust stages to an event-averaged analysis during dust–precipitation occurrences.

Because the original statement in Lines 361–362 was based on the previous analysis framework and is no longer consistent with the revised methodology and results, we have removed this sentence from the manuscript.

15. - Line 365:

Provide further discussion on the precipitation types in the cited papers (Wang et al., 2022; Zhu et al., 2023).

A: Thank you for this suggestion. We have clarified the precipitation regimes discussed in the cited studies.

Zhu et al., (2023) investigated the impacts of dust aerosols on both convective and stratiform precipitation over southeastern China during summer, and showed that under dusty conditions, precipitation tends to intensify in the mid-troposphere (−5 to +2 ℃) but weakens in both upper and lower layers, indicating an overall suppression of precipitation efficiency.

Wang et al. (2022b) is a review study. Rather than repeating its general conclusions, we directly discuss several observational studies summarized therein. For example, Min et al. (2009) analyzed a stratiform precipitation event associated with a trans-Atlantic Saharan dust outbreak and found that dust aerosols weakened precipitation intensity. Hui et al. (2008) showed that over the West African Sahel, dust aerosols suppress stratiform rainfall by increasing CCN concentrations and modifying the boundary-layer thermodynamic structure.

Overall, although these studies differ in region and season, they mainly involve stratiform precipitation systems. This is consistent with our study, which focuses on springtime dust–frontal precipitation over East Asia, where precipitation is predominantly stratiform. Therefore, these studies provide relevant observational support for our conclusions.

In Line 450-453:

Our results indicate that dust aerosols tend to suppress springtime dust-related precipitation over East Asia, where precipitation is predominantly stratiform. Similar suppression effects have also been reported in previous observational studies (Wang et al., 2022b; Zhu et al., 2023).

16. - Lines 426–427:

The statement “this study... mass concentrations” duplicates findings already reported by Park and Lim (2023).

A: Yes. We have corrected it.

We have removed the redundant statement and revised the text in Lines 510–513:

In order to explore the impact of spring dust aerosols on precipitation, in GRAPES/CUACE, we develop an on-line aerosol-IN nucleation scheme. The model performance has been evaluated by a typical dust-precipitation event from 00:00 UTC on 9 April to 00:00 UTC on 15 April 2018.

Related References

Bi, K., McMeeking, G. R., Ding, D. P., Levin, E. J. T., DeMott, P. J., Zhao, D. L., Wang, F., Liu, Q., Tian, P., Ma, X. C., Chen, Y. B., Huang, M. Y., Zhang, H. L., Gordon, T. D., and Chen, P.: Measurements of Ice Nucleating Particles in Beijing, China, Journal of Geophysical Research: Atmospheres, 124, 8065–8075, https://doi.org/10.1029/2019JD030609, 2019.

Chen, J., Wu, Z., Chen, J., Reicher, N., Fang, X., Rudich, Y., and Hu, M.: Size-resolved atmospheric ice-nucleating particles during East Asian dust events, Atmospheric Chemistry and Physics, 21, 3491–3506, https://doi.org/10.5194/acp-21-3491-2021, 2021.

Chen, Q., Yin, Y., Jiang, H., Chu, Z., Xue, L., Shi, R., Zhang, X., and Chen, J.: The Roles of Mineral Dust as Cloud Condensation Nuclei and Ice Nuclei During the Evolution of a Hail Storm, Journal of Geophysical Research Atmospheres, 124, https://doi.org/10.1029/2019JD031403, 2019.

Fang, W., Lou, X., Zhang, X., and Fu, Y.: Numerical Simulations of Cloud Number Concentration and Ice Nuclei Influence on Cloud Processes and Seeding Effects, Atmosphere, 13, 1792, https://doi.org/10.3390/atmos13111792, 2022.

Feng, Q., Niu, S., Niu, T., Fan, X., Shen, D., and Yang, J.: Aircraft—Based Observation of the Physical Characteristics of Snowfall Cloud in Shanxi Province, Chinese Journal of Atmospheric Sciences (in Chinese), 45, 1146–1160, 2021.

Filonchyk, M., Yan, H., Shareef, T. M. E., and Yang, S.: Aerosol contamination survey during dust storm process in Northwestern China using ground, satellite observations and atmospheric modeling data, Theor Appl Climatol, 135, 119–133, https://doi.org/10.1007/s00704-017-2362-8, 2019.

Gao, Q., Guo, X., He, H., Liu, X., Huang, M., and Ma, X.: Numerical Simulation Study on the Microphysical Characteristics of Stratiform Clouds with Embedded

Convections in Northern China based on Aircraft Measurements, Chinese Journal of Atmospheric Sciences (in Chinese), 44, 899−912, 2020.

He, C., Yin, Y., Huang, Y., Kuang, X., Cui, Y., Chen, K., Jiang, H., Kiselev, A., Möhler, O., and Schrod, J.: The Vertical Distribution of Ice-Nucleating Particles over the North China Plain: A Case of Cold Front Passage, Remote Sensing, 15, 4989, https://doi.org/10.3390/rs15204989, 2023.

Hong, S.-Y., Dudhia, J., and Chen, S.-H.: A Revised Approach to Ice Microphysical Processes for the Bulk Parameterization of Clouds and Precipitation, Monthly Weather Review, 132, 103–120, https://doi.org/10.1175/1520-0493(2004)132%253C0103:ARATIM%253E2.0.CO;2, 2004.

Hu, Y., Tian, P., Huang, M., Bi, K., Schneider, J., Umo, N. S., Ullmerich, N., Höhler, K., Jing, X., Xue, H., Ding, D., Liu, Y., Leisner, T., and Möhler, O.: Characteristics of ice-nucleating particles in Beijing during spring: A comparison study of measurements between the suburban and a nearby mountain area, Atmospheric Environment, 293, 119451, https://doi.org/10.1016/j.atmosenv.2022.119451, 2023.

Hui, W. J., Cook, B. I., Ravi, S., Fuentes, J. D., and D'Odorico, P.: Dust-rainfall feedbacks in the west african sahel, Water Resour. Res., 44, https://doi.org/10.1029/2008WR006885, 2008.

Igel, A. L., Igel, M. R., and Heever, S. C. van den: Make It a Double? Sobering Results from Simulations Using Single-Moment Microphysics Schemes, https://doi.org/10.1175/JAS-D-14-0107.1, 2015.

Jiang, H., Yin, Y., Wang, X., Gao, R., Yuan, L., Chen, K., and Shan, Y.: The measurement and parameterization of ice nucleating particles in different backgrounds of China, Atmospheric Research, 181, 72–80, https://doi.org/10.1016/j.atmosres.2016.06.013, 2016.

Kedzuf, N. J., Chiu, J. C., Chandrasekar, V., Biswas, S., Joshil, S. S., Lu, Y., van Leeuwen, P. J., Westbrook, C., Blanchard, Y., and O'Shea, S.: Retrieving microphysical properties of concurrent pristine ice and snow using polarimetric radar observations, Atmos. Meas. Tech., 14, 6885–6904, https://doi.org/10.5194/amt-14-6885-2021, 2021.

Lawson, R. P., Baker, B. A., Schmitt, C. G., and Jensen, T. L.: An overview of microphysical properties of arctic clouds observed in May and July 1998 during FIRE ACE, J. Geophys. Res.: Atmos., 106, 14989–15014, https://doi.org/10.1029/2000JD900789, 2001.

Min, Q.-L., Li, R., Lin, B., Joseph, E., Wang, S., Hu, Y., Morris, V., and Chang, F.: Evidence of mineral dust altering cloud microphysics and precipitation, Atmos. Chem. Phys., 9, 3223–3231, https://doi.org/10.5194/acp-9-3223-2009, 2009.

Molthan, A. L. and Colle, B. A.: Comparisons of Single- and Double-Moment Microphysics Schemes in the Simulation of a Synoptic-Scale Snowfall Event, https://doi.org/10.1175/MWR-D-11-00292.1, 2012.

Park, S.-Y. and Lim, K.-S. S.: Implementation of Prognostic Cloud Ice Number Concentrations for the Weather Research and Forecasting (WRF) Double-Moment 6-Class (WDM6) Microphysics Scheme, Journal of Advances in Modeling Earth Systems, 15, e2022MS003009, https://doi.org/10.1029/2022MS003009, 2023.

Pu, Z. and Lin, C.: Evaluation of double-moment representation of ice hydrometeors in bulk microphysical parameterization: comparison between WRF numerical simulations and UND-Citation data during MC3E, Geosci. Lett., 2, 11, https://doi.org/10.1186/s40562-015-0028-x, 2015.

Tobo, Y., Adachi, K., DeMott, P. J., Hill, T. C. J., Hamilton, D. S., Mahowald, N. M., Nagatsuka, N., Ohata, S., Uetake, J., Kondo, Y., and Koike, M.: Glacially sourced dust as a potentially significant source of ice nucleating particles, Nat. Geosci., 12, 253–258, https://doi.org/10.1038/s41561-019-0314-x, 2019.

Um, J., McFarquhar, G. M., Stith, J. L., Jung, C. H., Lee, S. S., Lee, J. Y., Shin, Y., Lee, Y. G., Yang, Y. I., Yum, S. S., Kim, B.-G., Cha, J. W., and Ko, A.-R.: Microphysical characteristics of frozen droplet aggregates from deep convective clouds, Atmospheric Chemistry and Physics, 18, 16915–16930, https://doi.org/10.5194/acp-18-16915-2018, 2018.

Wang, Y. and Yan, Z.: Effect of Different Verification Schemes on Precipitation Verification and Assessment Conclusion, Meteorological Monthly, 33, 9 (53-61), https://doi.org/10.3969/j.issn.1000-0526.2007.12.008, 2007.

Wang, Y., Kong, R., Cai, M., Zhou, Y., Song, C., Liu, S., Li, Q., Chen, H., and Zhao, C.: High small ice concentration in stratiform clouds over Eastern China based on aircraft observations: Habit properties and potential roles of secondary ice production, Atmospheric Research, 281, 106495, https://doi.org/10.1016/j.atmosres.2022.106495, 2023.

Wang, Z., Xue, L., Liu, J., Ding, K., Lou, S., Ding, A., Wang, J., and Huang, X.: Roles of Atmospheric Aerosols in Extreme Meteorological Events: a Systematic Review, Curr Pollution Rep, 8, 177–188, https://doi.org/10.1007/s40726-022-00216-9, 2022.

Yang, J., Hu, X., Lei, H., Duan, Y., Lv, F., and Zhao, L.: Airborne Observations of Microphysical Characteristics of Stratiform Cloud Over Eastern Side of Taihang Mountains, Chinese Journal of Atmospheric Sciences, 45(1), 88−106, 2021.

Zhang, M., Yu, H., Guo, J., Shen, X., Su, Y., Xue, H., and Dou, B.: Assessment on Unsystematic Errors of GRAPES_GFS 2.0, Journal of Applied Meteorological Science, 30, 332–344, 2019.

Zhang, Y., Yu, F., Luo, G., Fan, J., and Liu, S.: Impacts of long-range-transported mineral dust on summertime convective cloud and precipitation: a case study over the Taiwan region, Atmospheric Chemistry and Physics, 21, 17433–17451, https://doi.org/10.5194/acp-21-17433-2021, 2021.

Zhao, X., Lin, Y., Luo, Y., Qian, Q., Liu, X., Liu, X., and Colle, B. A.: A Double-Moment SBU-YLIN Cloud Microphysics Scheme and Its Impact on a Squall Line Simulation, Journal of Advances in Modeling Earth Systems, 13, e2021MS002545, https://doi.org/10.1029/2021MS002545, 2021.

Zhu, H., Li, R., Yang, S., Zhao, C., Jiang, Z., and Huang, C.: The impacts of dust aerosol and convective available potential energy on precipitation vertical structure in southeastern China as seen from multisource observations, Atmospheric Chemistry and Physics, 23, 2421–2437, https://doi.org/10.5194/acp-23-2421-2023, 2023.